THE JOURNAL OF PHYSICAL CHEMISTRY B

Article

pubs.acs.org/JPCB

Microscopic Hydration Properties of the $A\beta_{1-42}$ Peptide Monomer and the Globular Protein Ubiquitin: A Comparative Molecular Dynamics Study

Jaya C. Jose,[†] Prabir Khatua,[‡] Nupur Bansal,[†,§] Neelanjana Sengupta,*[,†] and Sanjoy Bandyopadhyay*[,‡]

[†]Physical Chemistry Division, CSIR-National Chemical Laboratory, Dr. Homi Bhaba Road, Pune 411008, India

[‡]Molecular Modeling Laboratory, Department of Chemistry, Indian Institute of Technology, Kharagpur 721302, India

Supporting Information

ABSTRACT: Atomistic molecular dynamics simulations of eight selected conformations of a disordered protein, amyloid beta (1−42) (Aβ), and a globular protein, ubiquitin (UBQ), have been carried out in aqueous media at 310 K. Detailed analyses were carried out to compare the microscopic properties of water molecules present in the hydration layers of these systems. It is noticed that irrespective of the conformational heterogeneity among the Aβ monomers, water molecules hydrating their surfaces exhibit relatively faster dynamics as compared to water molecules hydrating UBQ. Importantly, the conformational heterogeneity of the Aβ monomers has been found to affect the translational and rotational motions of hydration water molecules in a nonuniform manner. Detailed investigation of the timescale of hydrogen bond relaxations at the surface and their energetics revealed the possibility of heterogeneous confinement around different Aβ conformations. The distribution of water density fluctuation around Aβ conformations are broader compared to UBQ because of its predominant hydrophobic nature. Significant heterogeneity in the density fluctuation among the Aβ monomers suggests that the structural propensities could affect the peptide's effective surface hydrophobicity.

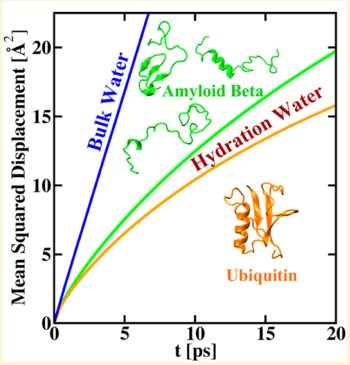

1. INTRODUCTION

Intrinsically disordered proteins (IDPs) belong to a class of protein sequences that do not possess uniquely folded native structures at physiological conditions.[1] The ability of IDPs to play important biological roles despite the absence of well-defined structure has defied the classic protein structure−function paradigm and triggered vast research on this protein subfamily.[2] The 4 kDa Amyloid beta (Aβ) peptide, which is created from enzymatic cleavage of the much larger membrane embedded precursor (APP) sequence and is strongly implicated in the onset of Alzheimer's disease (AD), has been considered a representative IDP system in recent studies.[3−5] While the "Amyloid hypothesis" implicates the peptide's fibrillar aggregates (known as "amyloids") in AD onset, emerging research indicates higher neurotoxicity of its soluble forms.[6] The full length Aβ peptide monomer adopts helical motifs in solvents with low polarity[7,8] but inhabits a wide conformational ensemble in the aqueous environment.[4,9,10] Aβ is thought to follow a nucleated polymerization mechanism, wherein a disordered, activated nucleus triggers the self-assembly pathway that eventually results in the formation of polymorphic protofibrillar and fibrillar aggregates.[11−13] Aβ is considered a paradigm for describing the conformational behavior for amyloidogenic proteins.[14]

Recent advances have significantly unraveled the physical origins of IDP behavior.[2] Among various key factors, the solvent environment has been found to have profound influence over the self-assembly behavior of proteins such as Aβ.[15] Alterations to the solvent environment can influence conformational flexibilities, structural ordering, and self-assembly kinetics of such disordered proteins.[8,16−18] In Aβ, interior hydration plays crucial roles in the stability of protofibrillar assemblies.[15,19,20] Further, the solvation free energy has been shown as an important component in the total free energy of dimerization of full length Aβ.[21]

Despite emerging knowledge on the role of solvent in the conformational and protein self-assembly behavior, little is known about the dynamical coupling of solvent molecules with the surface of disordered, assembly prone proteins such as Aβ. In contrast, hydration dynamics of natively folded proteins have been studied in great detail via advanced spectroscopic techniques and computer simulations.[22−28] In these systems, coupling with the protein surface causes marked deviations from bulk behavior in water molecules hydrating the surface. Their dynamical slowdown is reflected in their distinctly sublinear diffusion, longer tumbling times, and longer mean residence times in the hydration layer.[22−28] The water molecules hydrating the surface of a protein are often termed as "biological water",[29] due to their indispensable role in guiding the structure, dynamics, and, hence, function of the

Received: June 6, 2014
Revised: August 23, 2014
Published: September 8, 2014

   dx.doi.org/10.1021/jp505629q | J. Phys. Chem. B 2014, 118, 11591−11604

protein.[30] Importantly, it is shown that protein dynamical transitions and folding are "slaved" to solvent dynamics.[31,32] The anharmonic motions of the protein atoms have been found to be coupled to the hydrogen bond dynamics at the interface.[33] Recent work from our group showed that the conformational flexibility of key secondary structural elements of folded proteins affects the local heterogeneity in hydration water dynamics.[34,35]

As in the case of natively structured proteins, important signatures of solvent influences on an assembly prone protein can be obtained by exploring the extent of its dynamical coupling with the surrounding solvent layer. However, due to the inherent complex nature of the problem and lack of thermodynamically stable structures, no significant attempt has been made so far to explore the dynamical features of water molecules hydrating the surfaces of such proteins. To the best of our knowledge, the present study reports for the first time an in-depth analysis of the correlated dynamical behavior of water molecules hydrating an important protein in this class, namely, the Aβ peptide. We emphasize at this point that as the conformational ensembles of disordered proteins such as Aβ are widely distributed, it is essential to monitor the protein−water dynamical coupling of these systems by averaging of key properties over multiple representative conformations. Interestingly, in the case of globular proteins, it has been demonstrated recently that the distribution of reorientation dynamics of individual water molecules within the hydration shell and therefore the overall hydration shell dynamics are independent of the size and secondary structural contents of the proteins.[36] In this study, we have used atomistic molecular dynamics simulations to study key dynamical and energetic aspects of water molecules hydrating a variety of monomeric Aβ_{1-42} conformations. For comparison, we have performed equivalent analyses of solvent behavior on the surface of a folded globular protein, namely, ubiquitin (UBQ). Preliminary analysis with van Hove autocorrelation function suggests faster movement of surface water molecules in the Aβ ensemble over UBQ. Detailed analysis revealed a small but distinct shift toward bulk-like character of the hydration water molecules of Aβ over those of UBQ. However, the diffusion remained sublinear, while the rotational relaxation and the hydrogen bond dynamics were found to be significantly slower than that of bulk water, indicating strong protein−water dynamical coupling even in the structurally disordered Aβ. Overall, such differences in hydration layer behavior with UBQ appeared to be independent of the conformational characteristics of Aβ. Interestingly, however, the solvent on the Aβ surface displayed degrees of heterogeneity not associated with natively folded proteins. The rest of the article has been organized as follows. In System Setups and Simulation Protocols, we provide a brief description of the system setups and the simulation protocols employed. The results obtained from our analyses are presented and discussed in Results and Discussion. Finally, the important findings from the study, and the conclusions reached are highlighted in Conclusions.

2. SYSTEM SETUPS AND SIMULATION PROTOCOLS

Molecular Dynamics Simulations. Molecular dynamics (MD) simulations for eight different conformations of full length Aβ_{1-42} (AB1 to AB8) and ubiquitin (UBQ) were performed using NAMD2.8.[37] The methods used to generate the peptide conformations are described below. The CHARMM all atom force field with the CMAP correction was used.[38−40] The NH_3^+ and COO^- groups were added to the N- and C-termini of all the peptide and protein conformations. All the initial structures were solvated with TIP3P water molecules[41] followed by addition of counterions in order to afford charge neutral systems. The minimum distance from a protein atom to the edge of the simulation box was at least 14 Å. After 10000 steps of conjugate gradient energy minimization, 6 ns of simulations were carried out in the isothermal−isobaric (NPT) ensemble with orthorhombic periodic boundary conditions for equilibration of the systems. Constant temperature of 310 K was maintained with Langevin dynamics (collision frequency of 1 ps^{-1}), and the Langevin piston Nosé−Hoover method[42] maintained the constant pressure of 1 atm. The cutoff radius for the Lennard-Jones interactions was set to 12 Å. The SHAKE algorithm[43] was used for constraining bonds involving hydrogens. Electrostatic interactions were calculated with particle-mesh Ewald,[44] and a simulation time step of 1 fs was used. The equilibration was followed by 2 ns of simulations in the canonical (NVT) ensemble, with snapshots saved every 8 fs. These snapshots were used for all analyses presented in the study.

Ubiquitin. The initial structure of the 76 residue, natively folded protein Ubiquitin was taken from Protein Data Bank (PDB: 1UBQ).[45]

Aβ Conformations. Recent reports indicate that the Aβ monomeric ensemble is characterized by significant conformational heterogeneity.[4,9,46−50] Here, we point out that a recent study has shown that despite subtle differences in the isoforms, varying force fields largely converge in the important structural characteristics of the Aβ ensembles generated.[50] We generated a variety of full-length Aβ monomeric conformations with multiple methods that have been used widely for rapid sampling of protein conformational space, such as "replica exchange molecular dynamics" (REMD) and "accelerated molecular dynamics" (AMD).[48,50,51] The structure generation protocols are discussed in brief below. Keeping in mind the structural heterogeneity of the ensemble, eight individual Aβ conformations with varying secondary structural content were selected for our study. The structural basis of these selections, based on previous reports, is discussed in the next section.

The solution state NMR structure of Aβ_{1-42} peptide in a 70:30 mixture of water and hexafluoro-2-propanol has been reported in Protein Data Bank (PDB: 1Z0Q).[8] This structure is predominantly helical and has been used in several recent simulation studies.[52,53] This structure was simulated in the NPT ensemble for 150 ns, and the end-point conformation was designated as "AB1".

REMD[54] simulation method was carried out for the 1Z0Q structure, with 64 replicas spanning the temperature range from 330 to 600 K. Exchange time among the replicas was set to 0.25 ps, and the acceptance ratio was found to be greater than 10%. Each replica was simulated for 10 ns and hence the total simulation time was 640 ns. The Aβ conformations AB2, AB3, and AB4 were taken at the end point of the trajectories at 530, 600, and 594 K, respectively.

The 1Z0Q structure was simulated in the gas phase at a temperature of 373 K for 5 ns, generating several random coil conformations. A few snapshots were simulated in explicit water for up to 100 ns following the protocol described, and some were found to develop C-terminal β sheet character. Representative snapshots of a random coil conformation and one with C-terminal β sheet were designated AB5 and AB6, respectively.

AMD is a technique that ensures enhanced sampling of an ensemble in a short time by reducing the energy barrier between different states of the system. Details of the AMD technique are reported elsewhere.[51,55−57] Briefly, the system evolves in a modified potential, $V^*(\vec{r})$, which depends on the boost energy (E_b) and the acceleration parameter (α).

$$V^*(\vec{r}) = V(\vec{r}), \quad V(\vec{r}) \geq E_b \tag{1}$$

$$V^*(\vec{r}) = V(\vec{r}) + \Delta V(\vec{r}), \quad V(\vec{r}) < E_b \tag{2}$$

where the "bias potential" $\Delta V(r)$ is obtained as

$$\Delta V(\vec{r}) = \frac{[E_b - V(\vec{r})]^2}{E_b - V(\vec{r}) + \alpha} \tag{3}$$

AMD was performed on the 1Z0Q structure. The value of the dihedral boost, E_b, was fixed such that its difference with the mean dihedral energy in unbiased simulations was 4 kcal mol^{-1} times the number of residues in the peptide in accordance with recently optimized protocols.[57] The structure thus obtained was designated AB7.

A monomeric unit of a parallel β sheet structure was taken from the pentameric Aβ_{17-42} (PDB ID: 2BEG),[58] and the N-terminal sequence D_1AEFRHDSGYEVHHQK$_{16}$ generated with the VMD tool[59] in an extended orientation (dihedral angles, ψ = 180° and φ = 180°) was attached to get the full length Aβ_{1-42}. This conformation was simulated in the NPT ensemble for 5 ns and the end point designated as AB8.

3. RESULTS AND DISCUSSION

3.1. Characteristics of the Aβ Conformations. Aβ, unlike natively folded globular proteins, is characterized by large conformational fluctuations. Therefore, to probe the influence of the conformational heterogeneity of Aβ on its hydration layer, we have selected multiple monomeric conformations that describe the differential aspects of the Aβ conformational ensemble. We first note that helicity of the amyloid precursor protein (APP) is essential for its efficient enzymatic cleavage,[60] and thus nascent Aβ has been hypothesized to be in a helical conformation just after release into the aqueous cytoplasm.[8,47] The helical structure is also evident when solvents of lower polarity are added.[7,8] However, in pure aqueous solution, the ensemble is characterized by collapsed coil structure.[9,46] Extensive computer simulations indicate an enhanced probability for helicity at the N-terminal region[4] and a preferential antiparallel β sheet motif in the C-terminal region.[3,4,50] In Figure 1, we present representative snapshots of the Aβ conformations used in this study, along with a representative snapshot of UBQ conformation. The conformer AB1 is characterized by the highest degree of helicity in the N-terminal and turn regions and by the absence of any beta-sheet structure. In comparison to AB1, the conformations AB2, AB3, and AB4 have reduced helicities in the N-terminal and turn regions but a small extent of C-terminal helicity as reported earlier.[61] Among these three structures, AB2 is also characterized by the presence of an antiparallel β sheet in the C-terminal region. The conformation AB5 is predominantly characterized by the presence of turns and coils and has negligible helicity in the N-terminal region. While the helical conformations are completely absent in the AB6 conformation, there is a small extent of 3_{10} helicity in the N-terminal and turn regions. However, this conformation is characterized by the distinct presence of beta-sheet conformations in the central

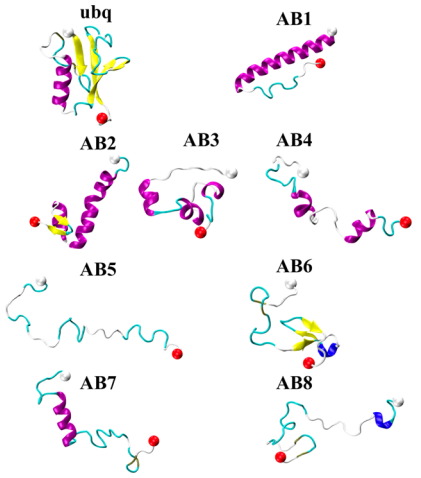

Figure 1. Representative snap shots of Aβ_{1-42} and UBQ from the simulated trajectories.

hydrophobic core ($F_{19}FA_{21}$) and in the C-terminal domains $K_{28}GAI_{31}$ and $M_{35}VGG_{38}$. We point out that the AB6 structure is comparable to the highly populated conformation reported in recent studies that plays significant roles in pathological aggregation of Aβ.[62,63] AB7 is also characterized by the presence of C-terminal beta-sheet and isolated bridge propensities, in addition to a reduced extent of N-terminal helicity in comparison to AB2. The AB8 conformation has marginal 3_{10} helicity in the N-terminal and turn regions but has distinct antiparallel beta-strands in the C-terminal region. In Table 1, we have presented the mean secondary structure percentages of the N-terminal, turn, and C-terminal domains of these conformations over the 2 ns analysis runs. In the Supporting Information, we have provided the residue-wise secondary structural content (Figure SI-1), root mean squared fluctuations (RMSF) of the non-hydrogen atoms (Figure SI-2 of the Supporting Information), and the mean values of the structural persistence, Q[64,65] (Text SI-1 and Table SI-1 of the Supporting Information). These analyses show that while the conformations are highly flexible, structural characteristics are conserved to a large extent during the analysis periods.

We further point out that conformational collapse of the Aβ monomer is considered a key early event in the peptide's self-assembly pathway.[46,47,66,67] Such compaction is attributed mainly to the interactions between key regions in the N- and C-terminal domains. In our earlier work, we have characterized the extent of Aβ compactness with the parameter "$d_{collapse}$", defined as the center of mass distance between the domains L_{17}VFFAEDVGS$_{26}$ and K_{28}GAIIGLMVGGVVIA$_{42}$.[65−67] In Table 2, we have listed the mean $d_{collapse}$ values over the trajectories of the eight Aβ conformations, along with the mean values of their radius of gyration (R_g) and the solvent accessible surface area per residue (SASA) calculated with VMD.[59] The SASA was obtained by calculating the total area covered by running a spherical probe of 1.8 Å radius over the peptide surface. As seen in Figure SI-3 of the Supporting Information, R_g and SASA are found to correlate reasonably well with the $d_{collapse}$ values. Despite their conformational differences, we find that the level of compactness of AB1, AB2, and AB6 are comparable. Interestingly, UBQ conformation has the lowest SASA and relatively low R_g values despite its longer sequence compared to Aβ, reflecting its high degree of compactness.

dx.doi.org/10.1021/jp505629q | J. Phys. Chem. B 2014, 118, 11591−11604

Table 1. Secondary Structure Details of Aβ Conformations; Average Secondary Structural Content (in Percentage) of the N- and C-Termini, and Turn Regions

secondary structure		Aβ conformations							
		AB1	AB2	AB3	AB4	AB5	AB6	AB7	AB8
N- terminus (res 1−21)	α-helix	97.02	78.62	37.05	24.74	0.0	0.0	51.46	0.0
	3_{10}-helix	0.0	0.02	0.03	0.80	0.21	3.14	5.07	1.43
	π-helix	0.0	0.0	0.0	1.10	0.0	0.0	0.0	0.0
	β-sheet	0.0	0.0	0.0	0.0	0.0	5.93	0.0	0.0
	isolated bridge	0.0	0.0	0.0	0.0	0.56	9.52	0.0	0.0
	turn and coil	2.98	21.36	62.92	73.36	99.22	81.41	43.47	98.57
turn (res 22−29)	α-helix	86.43	73.33	56.87	0.0	0.0	0.0	1.19	0.0
	3_{10}-helix	0.0	1.35	0.72	0.0	0.0	16.0	0.06	20.36
	π-helix	0.0	0.0	0.0	0.0	0.0	0.0	0.0	0.0
	β-sheet	0.0	0.0	0.0	0.0	0.0	16.34	0.0	0.0
	isolated bridge	0.0	0.0	0.0	0.0	0.0	0.78	0.0	0.0
	turn and coil	13.53	25.32	42.42	100.0	100.0	66.87	98.75	79.64
C-terminus (res 30−42)	α-helix	0.0	17.09	12.35	59.58	0.0	0.0	0.0	0.0
	3_{10}-helix	0.0	0.33	4.73	0.20	0.0	0.0	0.04	0.44
	π-helix	0.0	0.0	0.0	0.0	0.0	0.0	0.0	0.0
	β-sheet	0.0	30.52	0.0	0.0	0.0	34.09	6.42	0.0
	isolated bridge	0.0	0.12	0.0	0.0	0.0	2.47	11.54	12.25
	turn and coil	100.0	51.93	82.93	40.22	100.0	63.44	82.01	87.31

Table 2. Degree of Compactness and Interaction Strength with Hydration Water[a]

conf.	$<d_{collapse}>$	$<R_g>$	<SASA>	$<E_{tot\text{-}PW}>$
AB1	9.05	12.68	89.77	−4.49
AB2	10.38	12.12	90.12	−4.14
AB3	7.57	11.17	99.42	−4.04
AB4	23.60	18.58	114.26	−3.81
AB5	24.58	19.26	125.22	−3.64
AB6	5.94	11.70	93.41	−4.16
AB7	16.50	15.44	106.67	−3.78
AB8	10.90	14.82	109.73	−4.07
AB-avg	13.57	14.47	103.58	−4.02
UBQ	–	12.40	73.36	−5.42

[a]Average values of $d_{collapse}$ (in Å), R_g (in Å), SASA (in Å^2), and $E_{tot\text{-}PW}$ (in kcal mol^{-1}) for the Aβ Conformations and UBQ. Data Averaged Over the Eight Aβ Conformations are Specified as AB-avg.

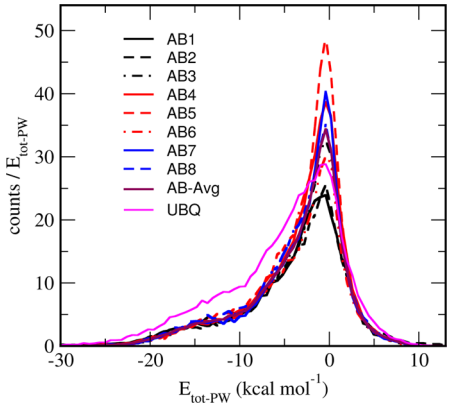

Figure 2. Distributions of the interaction energy ($E_{tot\text{-}PW}$) of the first hydration layer water molecules with the protein for different Aβ peptide conformations and UBQ. The corresponding distribution averaged over the Aβ monomers are also shown for comparison.

For a preliminary comparison and insights into the association of the hydration water molecules at the protein surface in the Aβ conformations and in UBQ, we have evaluated the total (i.e., electrostatic and van der Waals) interaction strengths, $E_{tot\text{-}PW}$, of individual water molecules residing in the hydration layer with the entire protein molecule. It may be noted here that all the calculations presented in the remaining manuscript are carried out by considering those water molecules that reside within a distance of 5 Å from the protein. This is consistent with earlier reports,[68] where it was shown that the effects of a protein on water properties are primarily restricted to the first hydration layer (within ∼5 Å). In Figure 2, we have presented the distributions of $E_{tot\text{-}PW}$, averaged over equispaced snapshots as obtained from the simulated trajectories and normalized such that the integrals of the distributions correspond to the total number of hydration water molecules.[28] As evident from the figure, the protein−water (PW) interactions are heterogeneous in nature, which agrees well with earlier reports.[28] However, the spread in $E_{tot\text{-}PW}$ in the Aβ conformations is found to be less compared to the corresponding distribution for UBQ. The mean values of the interaction strengths ($<E_{tot\text{-}PW}>$) are included in Table 2. We find that the PW interaction strengths on average are reduced by about 1.4 kcal mol^{-1} for the Aβ conformations as compared to UBQ. It may be noted here that compared to the Aβ monomers, more negative $<E_{tot\text{-}PW}>$ value or higher PW interaction strength for a tagged water present in the vicinity of UBQ is likely to arise due to its larger number of residues and more compact structure. However, we did not find any correlation between the mean total PW interaction strength with the overall secondary structure content and the degree of compactness of the Aβ conformations.

3.2. Dynamics of Hydration Water. *3.2.1. Translational Dynamics.* In this section, we explore and compare the microscopic dynamics of water molecules hydrating the Aβ monomers. The influence of heterogeneous conformations of the monomers and their flexibilities on the mobility of the nearby water molecules has been studied in detail. To assess and compare water translational dynamics, we first calculate the evolutions of the van Hove autocorrelation function $G_s(r, t)$ for those water molecules that were present initially ($t = 0$) in the

dx.doi.org/10.1021/jp505629q | J. Phys. Chem. B 2014, 118, 11591−11604

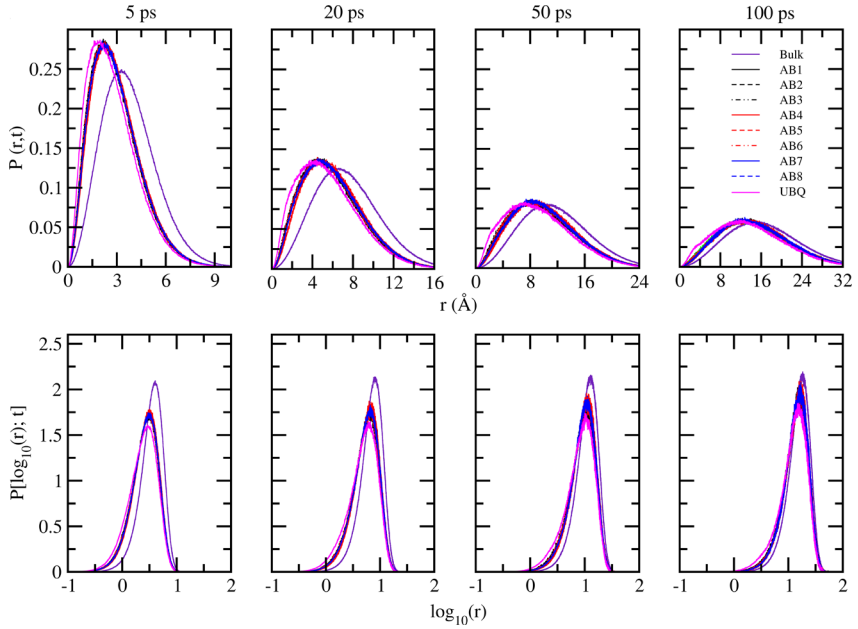

Figure 3. $P(r; t)$ as a function of r (top panel) and $P[\log_{10}(r); t]$ as a function of $\log_{10}(r)$ (bottom panel) for the first hydration layer water molecules around different Aβ peptide conformations and UBQ. As a reference, the corresponding functions for pure bulk water are included.

first hydration layers of the protein conformations. $G_s(r, t)$ is a space-time autocorrelation function which gives the probability density of finding a particle i at time t, if the particle was at the origin at $t = 0$. The function is defined for an N particle system as[68]

$$G_s(r, t) = \frac{1}{N}\sum_{i=1}^{N}\langle\delta[r + r_i(0) - r_i(t)]\rangle \quad (4)$$

where $r_i(t)$ denotes the position of the ith particle at time t. For purely homogeneous diffusion, $G_s(r, t)$ is a Gaussian function of the position r at all times t. In Figure 3 (upper panel), we present $4\pi r^2 G_s(r, t)$, or $P(r; t)$, the probability of a water molecule residing in the hydration layer at time $t = 0$, to have moved a distance r in time t at 5, 20, 50, and 100 ps, respectively. The calculations are carried out for water molecules around all the Aβ monomers and UBQ. As a reference, the corresponding data for pure bulk water as obtained from a separate MD simulation of TIP3P water under identical conditions is also included in the figure. Compared to water in pure bulk phase, slower diffusion of protein surface water at short times is evident from the figure. The results indicate near-identical mobility of water molecules around the Aβ monomers. However, compared to UBQ, small but noticeably higher mobility of water molecules hydrating the flexible Aβ molecules can be seen. It is known that for homogeneous diffusion, peak heights of the logarithm of the single particle displacement, $P[\log_{10}(r); t]$, calculated as $\ln(10)[4\pi r^3 G_s(r, t)]$, remains constant ($\sim$2.13) with time.[70,71] We have plotted $P[\log_{10}(r); t]$ versus $\log_{10}(r)$ for the hydration layer water molecules around all the protein systems, as shown in the lower panel of Figure 3. While the peak heights for bulk water remain nearly constant with time, they are distinctly lower for the protein hydration water, particularly at short times. It is evident that at shorter timescale (within a few tens of picoseconds), the water molecules exhibit constrained motions near the protein surface. In other words, a protein extends its influence on nearby water molecules for a duration up to a few tens of picoseconds. A closer examination of the data further reveals that while the peak heights for AB1 to AB8 are nearly the same, they are marginally higher compared to that observed for UBQ. This is an important finding that signifies that the water molecules around the flexible Aβ monomers tend to leave the first hydration layers relatively faster than those around the more compact globular UBQ. The peak positions in $P(r; t)$, and the peak heights in $P[\log_{10}(r); t]$ are provided in Table SI-2 of the Supporting Information.

It is evident from the above discussion that the water molecules hydrating the flexible Aβ monomers exhibit relatively faster mobility as compared to those around the globular protein UBQ. To obtain a more quantitative understanding of the effects of conformational heterogeneities of the Aβ conformers on the diffusive behavior of the hydration water molecules, we have directly probed water translational motions by calculating their mean square displacements (MSD), as a function of time. MSD is defined as,

$$\langle\Delta r^2\rangle = \langle|r_i(t) - r_i(0)|^2\rangle \quad (5)$$

where $r_i(t)$ and $r_i(0)$ are the position vectors of the oxygen atom of the i-th water molecule present in the first hydration layer at time t and at $t = 0$, respectively. The angular brackets denote that the averaging is carried out over different time origins and over the tagged water molecules. The calculations are carried out for water molecules around different Aβ monomers and UBQ, and the results are shown in Figure 4. The corresponding result for pure bulk water is included in the figure for comparison. We have also calculated water MSD averaged over all the Aβ monomers, as shown in the inset of the figure. It can be seen that compared to water in the pure bulk phase, translational motions of water molecules present in the hydration layers of conformationally disordered Aβ monomers and the globular UBQ are significantly restricted. Such restricted water motions at biomolecular interfaces are well-known.[35,69,72−74] Importantly, we notice that though water motions around the Aβ monomers are distinctly faster than that around UBQ, heterogeneity in solvent dynamical environment

dx.doi.org/10.1021/jp505629q | J. Phys. Chem. B 2014, 118, 11591−11604

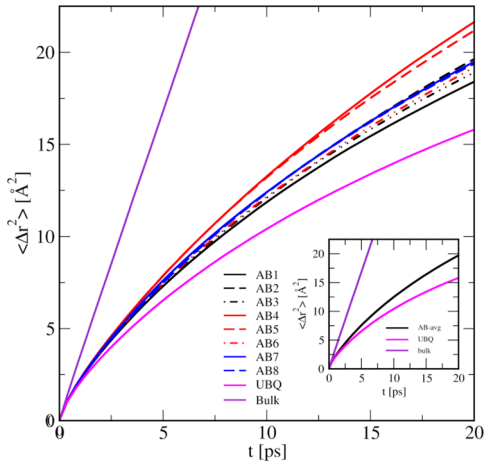

Figure 4. Mean square displacement (MSD) of water molecules present in the first hydration layers of different Aβ peptide conformations and UBQ. The MSD of water in pure bulk state is shown for comparison. The results for UBQ, pure bulk water, and that averaged over the Aβ monomers are also included in the inset.

exists around the Aβ conformations. The calculations reveal that although the differences are small, but among the 8 Aβ conformations studied, water molecules around AB1 exhibit the slowest and those around AB4 exhibit the fastest motions. It may be noted that unlike a globular protein, such as UBQ, Aβ being an IDP does not have a unique three-dimensional structure and exhibits fluctuations among different conformations separated by low-energy barriers under physiological conditions.[2,75] The present results along with the distributions of the van Hove function as discussed earlier (Figure 3) show that the intrinsic flexibility of Aβ and its frequent oscillations among different conformational states lead to a relatively more dynamic hydration layer around it as compared to that around UBQ. The results further suggest that the flexibility of Aβ leads to a nonuniform degree of confinement around its different conformations, thereby affecting the hydration water motions heterogeneously. We believe that the relatively more dynamic nature of the hydration layers around Aβ monomers is an important observation, as the water molecules in the vicinity of the monomers can then be easily displaced during the dewetting transition associated with the fibrillation process in amyloid pathology.[19]

We have calculated the diffusion coefficients (D_E) of water molecules hydrating the Aβ monomers and UBQ from the slopes of the corresponding MSD curves using Einstein's formulation,[76]

$$D_E = \lim_{\Delta t \to \infty} \frac{\langle \Delta r^2 \rangle}{2d\Delta t} \tag{6}$$

where d is the dimensionality of the system. The D_E values obtained along with that averaged over the Aβ monomers and for pure bulk water are listed in Table 3. It is apparent from the data that with respect to bulk water, the translational mobility of hydration water around UBQ is about 7 times slower, while the extent of retardation around the Aβ monomers is 4 to 5.5 times (average D_E value being 4.9 times lower). Besides, the water molecules around the Aβ monomers are found to diffuse on a timescale 23−60% faster than those around UBQ. Heterogeneous translational motions among the Aβ hydration water molecules are also evident from the data. We find that the water molecules around the AB4 monomer exhibit 30% faster translational mobility as compared to the slowest moving water around AB1. It may be noted that the diffusion of water in the vicinity of a large macromolecule is in general sublinear in nature.[69] Therefore, relative comparisons between the D_E values as discussed above are more meaningful than their absolute values.

Table 3. Translational Diffusion Coefficients (D_E) and Average Reorientational Time Constants ($\langle\tau_\mu\rangle$) of the First Hydration Layer Water Molecules Around Different Aβ Peptide Conformations and UBQ[a]

conf.	D_E (10^{-5} cm^2 s^{-1})	$\langle\tau_\mu\rangle$ (ps)
AB1	1.01	11.03
AB2	1.12	9.30
AB3	1.05	10.82
AB4	1.31	8.09
AB5	1.24	9.08
AB6	1.10	9.55
AB7	1.10	8.65
AB8	1.07	10.58
AB-avg	1.13 (0.05)	9.64 (0.46)
UBQ	0.82	13.50
bulk water	5.52	1.92

[a]The corresponding data averaged over the Aβ monomers (AB-avg) and that for pure bulk water are listed for comparison.

3.2.2. Rotational Dynamics. We now investigate the influence of heterogeneous conformational fluctuations of the Aβ peptide conformers on the rotational motions of water molecules hydrating their surfaces. Once again, the results are compared with that observed for the UBQ system. The calculations are carried out by measuring the timescale of reorientations of water dipoles, $\hat{\mu}$, defined as the unit vector connecting the oxygen atom of a water molecule to the center of the line joining the two hydrogen atoms. Time evolution of $\hat{\mu}$ has been studied by measuring the dipole−dipole time correlation function (TCF), $C_\mu(t)$, defined as

$$C_\mu(t) = \frac{\langle \hat{\mu}_i(0).\, \hat{\mu}_i(t) \rangle}{\langle \hat{\mu}_i(0).\, \hat{\mu}_i(0) \rangle} \tag{7}$$

Here, $\hat{\mu}_i(t)$ is the unit dipole moment vector of the ith water molecule at time t. Again, the calculations are carried out by averaging over the water molecules selected at different reference initial times. The results obtained for the water molecules hydrating the Aβ monomers and UBQ are displayed in Figure 5. For comparison, the result for pure bulk water is also included in the figure. $C_\mu(t)$ averaged over all the Aβ conformations are shown in the inset of the figure. First, it can be seen that the rotational motions of water molecules present in the first hydration layers around the Aβ monomers and the UBQ are significantly restricted. Consistent with the translational diffusion, the rotational motions of water molecules hydrating UBQ are also affected to a greater extent. Importantly, comparison of the results with those shown in Figure 4 reveals that the relative degree of heterogeneity in water rotational motions around different conformations of the Aβ peptide is similar to that noticed for their translational motions. Therefore, the conformational flexibility of the Aβ peptide affects both translational and rotational motions of hydration layer water molecules in a similar fashion.

dx.doi.org/10.1021/jp505629q | J. Phys. Chem. B 2014, 118, 11591−11604

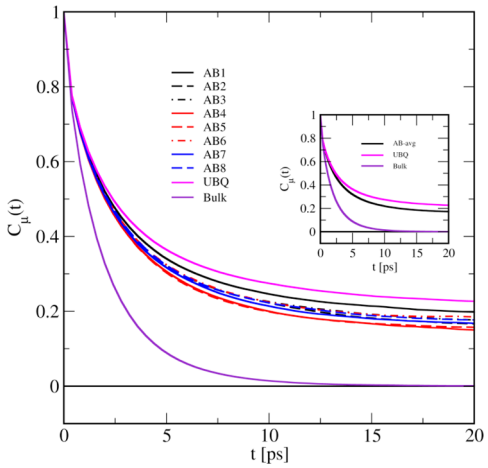

Figure 5. Reorientational time correlation function, $C_\mu(t)$, of water molecules present in the first hydration layers of different Aβ peptide conformations and UBQ. The corresponding function for water in pure bulk state is shown for comparison. The results for UBQ, pure bulk water, and that averaged over the Aβ monomers are also included in the inset.

The slow long-time decay of the $C_\mu(t)$ curves as evident from Figure 5 can be described by a multiexponential law. We have fitted each of the decay curves with triexponentials of the form,

$$C_\mu(t) = \sum_{i=1}^{3} A_i e^{-t/\tau_i} \quad (8)$$

where τ_i and A_i are the corresponding time constants and amplitudes, respectively. The amplitude-weighted average water reorientational times ($<\tau_\mu>$) as obtained from such fits for different Aβ monomers and UBQ are listed in Table 3. For comparison, the data for pure bulk water and that averaged over all the Aβ conformations are also listed in the table. Compared to water in the pure bulk state, significant longer duration taken by hydration water molecules to reorient themselves is clearly evident from the data. With respect to bulk water, we find that water molecules around UBQ take about 7 times longer to reorient, while those around the Aβ monomers take 4−6 times longer durations. However, the water molecules hydrating the flexible Aβ monomers reorient on a timescale 18−40% faster than that for UBQ. Once again, among the Aβ monomers, fastest and slowest water reorientations have been noticed around AB4 and AB1, respectively. A comparison between the D_E and the $<\tau_\mu>$ values provide evidence for near-identical relative influence of the Aβ monomers and UBQ on translational and rotational motions of hydration layer water molecules.

3.2.3. Role of Conformational Flexibility. One important issue in understanding the hydration behavior of a structurally disordered protein, such as Aβ, is the role played by its conformational flexibility on the microscopic properties of the surrounding water layer. We herein attempt to understand such role in the observed heterogeneity in the hydration layer behavior around different Aβ monomer conformations. For that, we have performed two additional simulations with the Aβ conformations whose hydration waters exhibit the fastest (AB4) and slowest (AB1) translational motions (see Figure 4), by restricting the peptide conformational flexibility with the application of harmonic restraints (2 kcal mol^{-1} Å^{-2}) to their nonhydrogen atoms. These simulations were carried out in the NVT ensemble for 2 ns, each following the same protocols as described earlier. In a recent study,[74] it is shown that even for a folded globular protein, loss of conformational flexibility leads to increasingly restricted hydration water motions. In light of this, the UBQ conformation was also similarly restrained and simulated. In Figure 6, we compare (a) the distributions of the

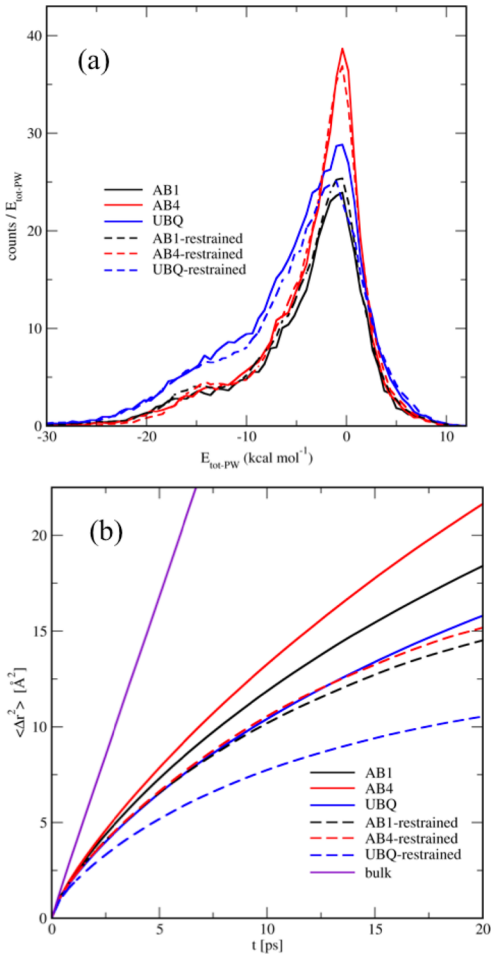

Figure 6. Comparison of (a) distributions of the total protein−water interaction strength, E_{tot-PW}, and (b) the mean square displacement (MSD) of the hydration layer water molecules, between the restrained and the flexible Aβ conformations AB1 and AB4, and those of UBQ. The MSD of water in pure bulk state is shown for comparison.

total PW interaction strength, E_{tot-PW}, and (b) the MSD, $<\Delta r^2>$, for the hydration layer water molecules, between the restrained and the unrestrained systems. As a reference, the data for pure bulk water are included in Figure 6b. It can be seen from the results (Figure 6a) that the loss in conformational flexibility has a relatively small effect on the net PW interaction strengths. This is evident from the calculated average interaction energies ($<E_{tot-PW}>$) as listed in Table 4. However, we notice that the absence of protein flexibility has a pronounced influence on the degree of restriction of the translational motions of water molecules hydrating the Aβ conformations as well as UBQ. This is consistent with our earlier work,[74] where the results show that irrespective of whether it is a globular protein or a disordered one, enhanced confinement at the surface on restraining the protein's flexibility results in increasingly restricted hydration water motions. Interestingly, it is found that though the hydration water molecules around restrained

dx.doi.org/10.1021/jp505629q | J. Phys. Chem. B 2014, 118, 11591−11604

Table 4. Average Protein−Water Interaction Strength ($<E_{tot\text{-}PW}>$), Translational Diffusion Coefficients (D_E) for the First Hydration Layer Water Molecules Around the Aβ Conformations AB1 and AB4, and UBQ in Restrained and Flexible Systems

type	conf.	$<E_{tot\text{-}PW}>$ (kcal mol^{-1})	D_E (10^{-5} cm^{2}s^{-1})
restrained	AB1	−4.48	0.72
	AB4	−3.60	0.76
	UBQ	−5.46	0.46
flexible	AB1	−4.49	1.01
	AB4	−3.81	1.31
	UBQ	−5.42	0.82

AB1 and AB4 exhibit increasingly retarded mobility, but the relative differences between those decrease significantly as compared to the corresponding flexible or unrestrained forms. It is clear that in the absence of conformational flexibility, the hydration environment around the Aβ monomers becomes nearly homogeneous. We have calculated the hydration water diffusion coefficients (D_E) following eq 6 for the restrained systems, which are listed in Table 4 along with the corresponding data for the flexible systems. Note that in the absence of conformational flexibility, water diffusivity close to the protein surface decreases by 30−45%. Further, the near-identical dynamic environment in the hydration layers of AB1 and AB4 in their restrained forms is clearly evident from the data. Our analysis clearly suggests that the relatively faster heterogeneous water motions around the Aβ monomers as compared to that around UBQ can largely be attributed to higher flexibility of the disordered Aβ conformers, rather than their relatively weaker interactions with surrounding solvent.

3.3. Hydrogen Bond Dynamics. It is clear from our discussion so far that the conformational disorders of the Aβ monomers affect the mobility of hydration water molecules in a heterogeneous manner. However, the water molecules around the fluctuating Aβ conformations exhibit translational and rotational motions on timescales relatively faster than that observed for water around more compact globular UBQ. Such heterogeneous influence of Aβ and UBQ on the dynamics of surrounding water molecules is expected to be coupled with the timescale associated with the formation and breaking of hydrogen bonds at the interface. We examine such influence in this section.

It is known that the presence of a macromolecule like a protein modifies the regular water−water (WW) hydrogen bond network in aqueous solution with the formation of protein−water (PW) hydrogen bonds.[35,69,74] Microscopic information on the dynamics of hydrogen bonds can be obtained from MD simulations through the calculation of different time correlation functions.[77−82] In this section, we investigate the hydrogen bond dynamics around different configurations of Aβ and compare the results with that observed for UBQ. To study hydrogen bonds, it is necessary to define them first. Either a geometry-based[79,82−85] or an energy-based criterion[41,81,86,87] is commonly used to define a hydrogen bond. In our calculations, we have used appropriate geometric criteria to define PW and WW hydrogen bonds. In this approach, the first condition to form a PW hydrogen bond is that the distance between the participating protein atom (donor or acceptor) and the oxygen atom of the tagged water be within 3.3 Å. The second condition for a protein acceptor atom (X) to form a PW hydrogen bond is that the angle between one of the O−H bond vectors of the water and the vector connecting the water oxygen and X be within 35°. Similarly, for a protein donor atom (Y) to form such hydrogen bond, the angle between Y−H bond vector and the vector connecting Y and the water oxygen should be within 35°. Besides, two water molecules are considered to be hydrogen bonded if their interoxygen and nonbonded oxygen−hydrogen distances are within 3.5 and 2.45 Å, respectively, and the oxygen−oxygen−hydrogen angle is less than 30°.[79,82,85]

We have investigated the dynamics of hydrogen bonds by calculating two time correlation functions (TCF), namely, the intermittent hydrogen bond TCF [$C(t)$] and the continuous hydrogen bond TCF [$S(t)$]. The two functions are defined as[77,78,87]

$$C(t) = \frac{\langle h(0)h(t)\rangle}{\langle h(0)h(0)\rangle} \tag{9}$$

and

$$S(t) = \frac{\langle h(0)H(t)\rangle}{\langle h(0)h(0)\rangle} \tag{10}$$

The definitions are based on two population variables $h(t)$ and $H(t)$. The variable $h(t)$ is considered to be unity if a particular pair of sites (PW or WW) are hydrogen-bonded at time t, and zero, otherwise. On the other hand, $H(t)$ is defined as unity when a particular pair of sites remain continuously hydrogen bonded from time $t = 0$ to a later time t, and zero, otherwise. The angular brackets indicate that the averaging is carried out over all the hydrogen bonds of a particular type (PW or WW) at different time origins. In accordance with the definitions, $C(t)$ corresponds to the probability that a particular hydrogen bond formed at time $t = 0$ will be found intact at a later time t. It is therefore independent of the history of breaking and reformation of hydrogen bonds at intermediate times. Thus, recrossing of the barrier between the bonded and the nonbonded states and the long-time diffusive behavior are included in $C(t)$. Therefore, $C(t)$ can provide information on the timescale of overall hydrogen bond structural reorganization at the interface. The function $S(t)$, on the other hand, describes the probability that a particular hydrogen bond formed at $t = 0$ remains continuously intact at all times up to t. Hence, $S(t)$ provides a true estimate of the lifetime or the survival time of a hydrogen bond.

We first calculate the intermittent hydrogen bond TCF [$C_{PW}(t)$] for the PW hydrogen bonds formed by the residues of the Aβ monomers and UBQ with water molecules at their surfaces, as shown in Figure 7a. In Figure 7b, we show the relaxation patterns of $C_{WW}(t)$ corresponding to the WW hydrogen bonds formed by the first hydration layer water molecules around the proteins. In the insets, we compare the relaxations of $C_{PW}(t)$ and $C_{WW}(t)$ averaged over all the Aβ conformations with that obtained for UBQ. As a reference, the decay of $C_{WW}(t)$ for WW hydrogen bonds in pure bulk water is included in both the figures. It is evident from the results that regardless of whether the hydration water molecules are involved in PW or WW hydrogen bonds, the relaxations of $C(t)$ are always slower with longer relaxation times than that of bulk water, the effect being more prominent for the PW hydrogen bonds. Such slower relaxations of hydrogen bonds involving the first hydration layer water molecules correlate well with their restricted translational and rotational motions, as discussed earlier (see Figures 4 and 5). Importantly, the

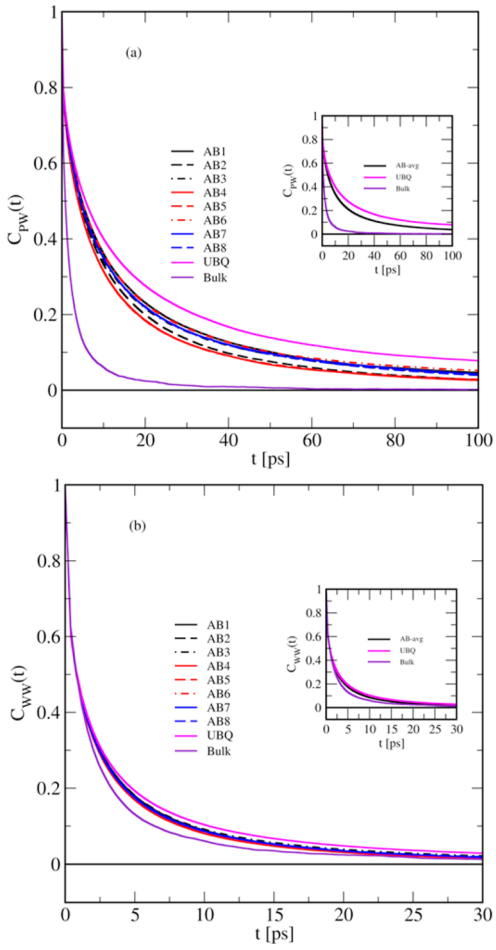

Figure 7. (a) Intermittent time correlation function, $C_{PW}(t)$, for the PW hydrogen bonds formed between water molecules and the residues of different Aβ peptide conformations and UBQ. (b) The corresponding function, $C_{WW}(t)$, for the WW hydrogen bonds formed by the first hydration layer water molecules around different Aβ peptide conformations and UBQ. The function $C_{WW}(t)$ for water in pure bulk state is shown for comparison. The results for UBQ, pure bulk water, and that averaged over the Aβ monomers are also included in the insets.

relaxation of PW hydrogen bonds formed by the UBQ residues is noticeably slower than that corresponding to the Aβ monomers (Figure 7a). Besides, a heterogeneous timescale of PW hydrogen bond relaxation among different Aβ monomers is evident from the data. Interestingly, the WW hydrogen bonds formed by the first hydration layer water molecules around the Aβ monomers exhibit near-homogeneous dynamics that are marginally faster than those around UBQ, as observed in Figure 7b. This is an important finding, which shows that the heterogeneous motions of water molecules present in the first hydration layers of the Aβ monomers as discussed earlier correlate well with slow nonuniform relaxations of PW hydrogen bonds formed at the protein surfaces. Note that such nonuniform relaxations of PW hydrogen bonds among the Aβ monomers once again confirm heterogeneous degree of confinement around their fluctuating configurations. To obtain estimates of the PW and WW hydrogen bond relaxation times, we have once again fitted each of the decay curves in Figure 7 with triexponentials (eq 8). The amplitude-weighted average relaxation times ($<\tau_c^{PW}>$ and $<\tau_c^{WW}>$) as obtained from such fits are listed in Table 5. For comparison, the corresponding

Table 5. Average Relaxation Times as Obtained from the Intermittent PW ($<\tau_c^{PW}>$) and WW ($<\tau_c^{WW}>$) Hydrogen Bond TCFs for the Water Molecules Present in the First Hydration Layers around Different Aβ Peptide Conformations and UBQ[a]

conf.	$<\tau_c^{PW}>$ (ps)	($<\tau_c^{WW}>$) (ps)
AB1	18.06	3.27
AB2	14.58	3.21
AB3	17.02	3.42
AB4	13.63	3.07
AB5	13.49	3.10
AB6	19.03	3.23
AB7	17.72	3.23
AB8	16.95	3.30
AB-avg	16.31 (0.99)	3.23 (0.05)
UBQ	24.86	3.83
bulk water	–	2.93

[a]The corresponding data averaged over the Aβ monomers (AB-avg) and that for pure bulk water are listed for comparison.

value for pure bulk water and that obtained by averaging over all the Aβ monomers are also listed in the table. It is clear from the data that compared to bulk water, the PW hydrogen bonds take longer durations to relax. In particular, the average relaxation time of PW hydrogen bonds formed by UBQ is 8.5 times more than bulk water, whereas the corresponding hydrogen bonds formed by the Aβ monomers take 4.5−6.5 times longer to relax. Significant heterogeneity in PW hydrogen bond environment around the flexible Aβ monomers is also evident from the corresponding $<\tau_c^{PW}>$ values. Note that compared to the PW hydrogen bonds, the WW hydrogen bonds formed by the first hydration layer water molecules take only marginally longer times (~30% longer for UBQ and 5−17% for Aβ monomers) to relax than that for water in the pure bulk state.

In Figure 8, we show the relaxations of continuous hydrogen bond TCFs [$S_{PW}(t)$ and $S_{WW}(t)$] corresponding to the PW and WW hydrogen bonds around the Aβ monomers and UBQ. The data averaged over all the Aβ conformations have also been calculated as shown in the insets. The result for pure bulk water is once again included in the figure as a reference. It can be seen from Figure 8a that for each system, the function $S_{PW}(t)$ relaxes slowly as compared to bulk water, thereby indicating longer lifetimes of PW hydrogen bonds. Interestingly, unlike $C_{PW}(t)$, we do not observe any distinct difference in the relaxation patterns of $S_{PW}(t)$ between the Aβ monomers among themselves and that between UBQ and Aβ. The $S_{WW}(t)$ decay curves for the WW hydrogen bonds involving the hydration water molecules show even more interesting behavior. It is evident from Figure 8b that compared to bulk water, the function relaxes noticeably slowly for UBQ. On the other hand, the results for water around the Aβ monomers are found to be almost indistinguishable from that of water in the pure bulk state. Again, we have fitted each of the $S_{PW}(t)$ and $S_{WW}(t)$ decay curves with triexponentials (eq 8) and calculated the amplitude-weighted average lifetimes of the PW and WW hydrogen bonds ($<\tau_s^{PW}>$ and $<\tau_s^{WW}>$), which are listed in Table 6. As before, the lifetime of WW hydrogen bonds in pure bulk state and that obtained by averaging over all the Aβ monomers are also listed in the table. It can be seen that compared to bulk water, the PW hydrogen bonds in general exhibit 2−3 times longer lifetimes. On the other hand, though

dx.doi.org/10.1021/jp505629q | J. Phys. Chem. B 2014, 118, 11591−11604

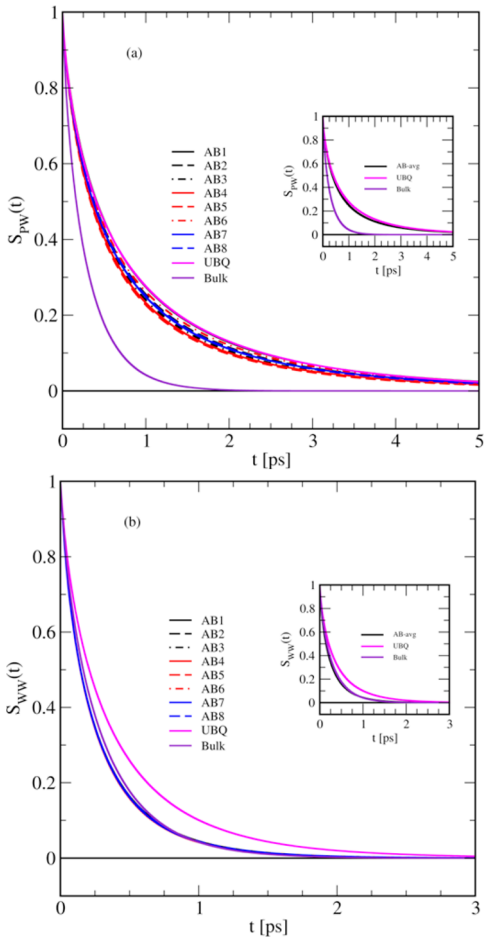

Figure 8. (a) Continuous time correlation function, $S_{PW}(t)$, for the PW hydrogen bonds formed between water molecules and the residues of different Aβ peptide conformations and UBQ. (b) The corresponding function, $S_{WW}(t)$, for the WW hydrogen bonds formed by the first hydration layer water molecules around different Aβ peptide conformations and UBQ. The function $S_{WW}(t)$ for water in pure bulk state is shown for comparison. The results for UBQ, pure bulk water, and that averaged over the Aβ monomers are also included in the insets.

the WW hydrogen bonds around globular UBQ survive ~40% longer since their formations, there is hardly any distinction between the WW hydrogen bond survival times in the hydration layers of the Aβ monomers and that in the pure bulk state.

Let us attempt to explain the origin of the heterogeneous influence of the proteins on the relaxations of intermittent and continuous hydrogen bond TCFs, as observed above. We already mentioned that the functions $S_{PW}(t)$ and $S_{WW}(t)$ provide absolute estimates of the average durations over which PW and WW hydrogen bonds would survive due to their formations and are independent of water translational and rotational motions. Therefore, the relaxation timescales of these functions should depend on hydrogen bond strengths. Using the definitions of hydrogen bonds, we have calculated the average interaction energy between a water molecule and the residue of the protein (Aβ or UBQ) (E_{PW}) with which it is hydrogen-bonded. Similarly, the average interaction energy of a pair of hydrogen-bonded water molecules (E_{WW}) present either in the hydration layer or in the bulk state is also computed. The calculated values are listed in Table 6. The energy values averaged over the Aβ monomers are also listed for comparison. It can be seen that on average a PW hydrogen bond is about 2 times stronger than a WW hydrogen bond. Therefore, a PW hydrogen bond once formed at the surface of a protein (Aβ or UBQ) survives longer than a WW hydrogen bond due to its greater strength. Interestingly, we notice that despite identical residue sequence, as observed in the case of average total interaction energy between a water molecule in the hydration layer and the protein surface, the PW hydrogen bond strengths among the Aβ monomers are noticeably different (within 10% with respect to the average value). It is known that appropriate geometrical orientation between a residue and a water molecule is necessary to form a PW hydrogen bond. The results indicate that due to heterogeneous conformational features of the Aβ monomers and the degree of confinement around them, the relative orientations of PW hydrogen-bonded pairs are different. As a result, the PW hydrogen bond strengths and hence their average lifetimes differ among the Aβ monomers. Note that unlike $<E_{tot\text{-}PW}>$ (see Table 2), $<E_{PW}>$ is independent of the size or the number of residues of the protein. However, due to the different primary amino acid sequence and their types, $<E_{PW}>$ values between Aβ and UBQ

Table 6. Average Relaxation Times as Obtained From the Continuous PW ($<\tau_s^{PW}>$) and WW ($<\tau_s^{WW}>$) Hydrogen Bond TCFs for the Water Molecules Present in the First Hydration Layers Along with the Average Interaction Energy Between a Protein Residue and a Water Molecule Hydrogen-Bonded to It ($<E_{PW}>$) and that between a Pair of Hydrogen-Bonded Water Molecules ($<E_{WW}>$) around Different Aβ Peptide Conformations and UBQ[a]

conf.	$<\tau_s^{PW}>$ (ps)	($<\tau_s^{WW}>$) (ps)	($<E_{PW}>$) (kcal/mol)	($<E_{WW}>$) (kcal/mol)
AB1	0.88	0.27	−8.43	−4.08
AB2	0.83	0.27	−8.26	−4.08
AB3	0.75	0.27	−7.52	−4.08
AB4	0.67	0.27	−7.35	−4.08
AB5	0.56	0.27	−7.15	−4.08
AB6	0.85	0.27	−7.54	−4.08
AB7	0.79	0.27	−7.69	−4.08
AB8	0.82	0.27	−7.39	−4.08
AB-avg	0.77 (0.05)	0.27	−7.67 (0.21)	−4.08
UBQ	0.89	0.39	−8.18	−4.06
bulk water	–	0.28		−4.20

[a]The corresponding data averaged over the Aβ monomers (AB-avg) and that for pure bulk water are listed for comparison.

dx.doi.org/10.1021/jp505629q | J. Phys. Chem. B 2014, 118, 11591−11604

are to a small extent different with PW hydrogen bonds formed by UBQ being marginally stronger than those formed by Aβ. In contrast to the PW hydrogen bonds, we notice identical hydrogen-bonded water pair interaction energy, similar to that for the bulk state, around the Aβ monomers. This is reflected in identical bulk-like WW hydrogen bond lifetimes around them. Surprisingly, despite similar WW hydrogen bond energy near UBQ, these hydrogen bonds survive over relatively longer durations as mentioned before. We believe that such differences in WW hydrogen bond lifetimes around UBQ and Aβ monomers arise due to heterogeneous confinement around them. As already discussed, UBQ with more compact secondary structures can confine hydrogen-bonded water molecules present in its hydration layer more effectively than the disordered Aβ conformations. As a result, hydration layer water molecules around UBQ although form WW hydrogen bonds of similar strength, but they survive over longer periods.

It may be noted that the hydrogen bond properties often depend on their definitions. To verify such dependence on WW hydrogen bond lifetimes, if any, we have recalculated the function $S_{WW}(t)$ for the hydration water molecules around the Aβ monomers and UBQ using an energy-based criterion[87] to define such bonds. The details of the criterion and the results as obtained have been provided in Text SI-2, Figure SI-4, and Table SI-3 of the Supporting Information. Comparison of the results with that discussed above (Figure 8b and Table 6) clearly shows that the relaxation patterns of $S_{WW}(t)$ and hence the lifetimes of WW hydrogen bonds ($<\tau_s^{WW}>$) around the Aβ monomers are nearly independent of their definition. In contrast, however, we notice that the average WW hydrogen bond lifetime around UBQ depends on the criterion used to define those bonds. In fact, the energy-based criterion leads to relatively shorter $<\tau_s^{WW}>$ in the hydration layer of UBQ, which becomes the same as that obtained around the Aβ conformations (Table SI-3 of the Supporting Information). It is clear from the results that the energy-based criterion avoids the influence of nonuniform confinement around the flexible Aβ conformations and compact UBQ as observed in Figure 8b. This is an important observation which, however, needs to be investigated further.

3.4. Water Density Fluctuations. Before concluding, we attempt to obtain preliminary insights into how the observed nonuniform hydration behavior between the Aβ conformers and UBQ are correlated with the nature of the protein surface. Recent research shows a close association of the water density fluctuations in the vicinity of a surface with the physicochemical nature of the surface.[88−90] It has been shown that water densities within small probe volumes in close vicinity of a surface have Gaussian distributions whose widths increase with increasing surface hydrophobicity. In the case of biomolecules, enhanced water density fluctuation near hydrophobic surfaces can alter interactions and functions.[90] As hydrophobicity plays important roles in the behavior of Aβ,[13,19,66] it may therefore be worthwhile to compare water density fluctuations close to the surface of the Aβ conformers with those around UBQ. From our simulation snapshots, we obtained the water number densities within a probe volume approximated as the product of the SASA and 3 Å. For ease of comparison, we obtained $P(n^*)$, which is the probability distribution of the water number density divided by the mean density, n^*, normalized by the maximum probability. In Figure 9, we have plotted $P(n^*)$ as a function of n^* fitted to the Gaussian form,

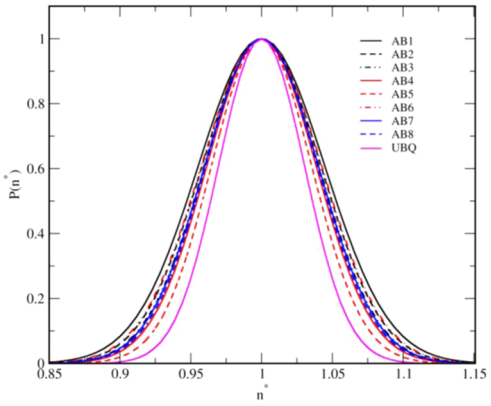

Figure 9. Probability distributions of water densities near the surfaces of different Aβ peptide conformations and UBQ fitted to the Gaussian form. See text for details.

$$P(n^*) = e^{-\frac{(n^*-1)^2}{\alpha}} \tag{11}$$

We have listed the values of α for each of the Aβ conformers and UBQ in Table SI-4 of the Supporting Information. The distribution corresponding to each Aβ conformer is found to be broader than that obtained for UBQ, demonstrating the overall higher surface hydrophobicity of the Aβ sequence. Interestingly, the water density distributions of the individual Aβ conformations are not identical, with the distributions being marginally narrower for the conformations with lower secondary structural content. This analysis suggests that the conformational propensities are associated with both surface hydrophobicity as well as the dynamical behavior of the hydration layer. Further investigations that develop and employ more rigorous definitions of the probe volume could help reveal the interplay of conformational fluctuations and surface hydrophobicity and their relationship with the hydration layer behaviors of disordered proteins.

4. CONCLUSIONS

In this article, we have analyzed the microscopic association of the protein hydration layer with putative Aβ conformations and with the natively folded state of ubiquitin (UBQ), a small globular protein, using atomistic MD simulations. Compared to UBQ, the Aβ monomers demonstrate marginally weaker association with the hydration layer. Detailed analyses of the dynamical behavior of the hydration layers show that the water molecules hydrating the Aβ conformations exhibit faster translational and rotational motions compared to those hydrating UBQ. The heterogeneous motions of the Aβ hydration water molecules are found to be correlated with the relaxation timescales of protein−water (PW) and water−water (WW) hydrogen bonds at the interfaces. It is demonstrated that though the average survival time of a PW hydrogen bond around Aβ and UBQ are nearly the same, the nonuniform influence of the two proteins on water dynamics leads to heterogeneous timescales of overall structural relaxation of PW hydrogen bonds. Further, it is found that the structural variation in Aβ leads to changes in the hydration layer dynamics. Thus, conformational fluctuations and alterations in the degree of surface exposure can affect coupling of the Aβ peptide with the hydration layer and lead to an overall increase in the heterogeneous behavior of the hydration water molecules.

dx.doi.org/10.1021/jp505629q | J. Phys. Chem. B 2014, 118, 11591−11604

Our results are of biological significance in studies of Aβ self-assembly, where hydration water has been shown to play crucial roles in early oligomeric assembly and in protofibrillar stability.[15,19] The entropic contribution of the hydration waters upon release into the bulk phase is one of the key factors that drive early self-assembly.[21,91,92] Thus, the relative effects of the protein surface on the dynamical behavior of its surrounding water molecules could be an important indicator of its aggregation propensity. However, it remains to be investigated if the observed differences relative to a folded protein are representative of general IDP hydration or is unique to the Aβ peptide. This will require further studies of microscopic hydration properties of multiple IDP sequences of varying surface topology and detailed investigations of how the key domains associated with their self-assembly influence local as well as overall hydration dynamics. Some of these aspects are under active investigation in our laboratory.

■ ASSOCIATED CONTENT

Supporting Information

(Figure SI-1) Residue-wise secondary structural content during the 2 ns analysis run for the eight Aβ conformations. (Figure SI-2) Root-mean-squared fluctuations (RMSF) of all the nonhydrogen atoms during the 2 ns analysis run for the eight Aβ conformations. (Text SI-1) Details of structural persistence. (Table SI-1) Structural persistence, Q, averaged over the 2 ns analysis runs for the eight Aβ conformations. Standard deviations are provided in parentheses. The high Q values indicate that the secondary structures are largely conserved during this period. (Figure SI-3) (a) Average $d_{collapse}$ versus average SASA and (b) average $d_{collapse}$ versus average R_g of different Aβ peptide conformations. (Table SI-2) Peak positions of $P[(r); t]$ and peak heights of $P[\log_{10}(r); t]$ (in Å) for the first hydration layer water molecules around different Aβ peptide conformations and UBQ. As a reference, the corresponding data for pure bulk water are also listed. (Text SI-2) Energy-based definition of WW hydrogen bonds. (Figure SI-4) Continuous time correlation function, $S_{WW}(t)$, as calculated using the energy-based criterion to define WW hydrogen bonds formed by the first hydration layer water molecules around different Aβ peptide conformations and UBQ. $S_{WW}(t)$ for water in pure bulk state is shown for comparison. The results for UBQ, pure bulk water, and that averaged over the Aβ monomers are also included in the inset. (Table SI-3) Average relaxation times as obtained from the continuous WW ($<\tau_s^{WW}>$) hydrogen bond TCFs (calculated using the energy-based criterion) for the water molecules present in the first hydration layers around different Aβ peptide conformations and UBQ. The corresponding data averaged over the Aβ monomers (AB-avg) and that for pure bulk water are listed for comparison. (Table SI-4) The values of α obtained from fits of the water density distribution $P(n^*)$ to eq 11 for the Aβ peptide conformations and UBQ. (List SI-1): The Complete Author List for refs 10 and 40. This material is available free of charge via the Internet at http://pubs.acs.org.

■ AUTHOR INFORMATION

Corresponding Authors

*E-mail: n.sengupta@ncl.res.in.

*E-mail: sanjoy@chem.iitkgp.ernet.in.

Present Address

[§]N.B.: Department of Chemistry, Michigan State University, East Lansing, MI 48824, United States.

Notes

The authors declare no competing financial interest.

■ ACKNOWLEDGMENTS

N.S. acknowledges funding provided through the CSIR 12th Five Year Plan Project: Multi-Scale Simulation and Modeling project (or MSM; project number CSC0129). J.C.J. thanks CSIR for her senior research fellowship and Asis K. Jana for the random coil simulations of Aβ. This study was supported in part by grants from the Department of Science and Technology (DST) (SR/S1/PC-23/2007), Government of India. Part of the work was carried out using the computational facilities created under the DST-FIST programme (SR/FST/CSII-011/2005) and DST-IYC award. P.K. thanks the University Grants Commission (UGC), Government of India, for providing a scholarship. N.S. would like to thank Dr. Sarika Bhattacharyya for discussions.

■ REFERENCES

(1) Dyson, H. J.; Wright, P. E. Intrinsically Unstructured Proteins and Their Functions. *Nat. Rev. Mol. Cell Biol.* **2005**, *6*, 197−208.

(2) Tompa, P. Intrinsically Disordered Proteins: A 10-Year Recap. *Trends Biochem. Sci.* **2012**, *37*, 509−516.

(3) Ball, K. A.; Phillips, A. H.; Nerenberg, P. S.; Fawzi, N. L.; Wemmer, D. E.; Head-Gordon, T. Homogeneous and Heterogeneous Tertiary Structure Ensembles of Amyloid-β Peptides. *Biochemistry* **2011**, *50*, 7612−7628.

(4) Lin, Y.-S.; Bowman, G. R.; Beauchamp, K. A.; Pande, V. S. Investigating How Peptide Length and a Pathogenic Mutation Modify the Structural Ensemble of Amyloid Beta Monomer. *Biophys. J.* **2012**, *102*, 315−324.

(5) Fisher, C. K.; Ullman, O.; Stultz, C. M. Comparative Studies of Disordered Proteins with Similar Sequences: Application to Aβ40 and Aβ42. *Biophys. J.* **2013**, *104*, 1546−1555.

(6) Haass, C.; Selkoe, D. J. Soluble Protein Oligomers in Neurodegeneration: Lessons from the Alzheimer's Amyloid β-Peptide. *Nat. Rev. Mol. Cell Biol.* **2007**, *8*, 101−112.

(7) Crescenzi, O.; Tomaselli, S.; Guerrini, R.; Salvadori, S.; D'Ursi, A. M.; Temussi, P. A.; Picone, D. Solution structure of the Alzheimer Amyloid B-Peptide (1−42) In An Apolar Microenvironment. *Eur. J. Biochem.* **2002**, *269*, 5642−5648.

(8) Tomaselli, S.; Esposito, V.; Vangone, P.; van Nuland, N. A.; Bonvin, A. M.; Guerrini, R.; Tancredi, T.; Temussi, P. A.; Picone, D. The Alpha-to-Beta Conformational Transition of Alzheimer's Abeta-(1−42) Peptide in Aqueous Media is Reversible: a Step by Step Conformational Analysis Suggests the Location of Beta Conformation Seeding. *ChemBioChem* **2006**, *7*, 257−267.

(9) Sgourakis, N. G.; Yan, Y.; McCallum, S. A.; Wang, C.; García, A. E. The Alzheimer's Peptides Aβ 40 and 42 Adopt Distinct Conformations in Water: A Combined MD/NMR Study. *J. Mol. Biol.* **2007**, *368*, 1448−1457.

(10) Hou, L.; Shao, H.; Zhang, Y.; Li, H.; Menon, N. K.; Neuhaus, E. B.; Brewer, J. M.; Byeon, I.-J. L.; Ray, D. G.; Vitek, M. P.; et al. Solution NMR Studies of the Aβ(1−40) and Aβ(1−42) Peptides Establish that the Met35 Oxidation State Affects the Mechanism of Amyloid Formation. *J. Am. Chem. Soc.* **2004**, *126*, 1992−2005.

(11) Massi, F.; Straub, J. E. Energy Landscape Theory for Alzheimer's Amyloid B-Peptide Fibril Elongation. *Proteins: Struct., Funct., Bioinf.* **2001**, *42*, 217−229.

(12) Pellarin, R.; Caflisch, A. Interpreting the Aggregation Kinetics of Amyloid Peptides. *J. Mol. Biol.* **2006**, *360*, 882−892.

(13) Reddy, G.; Straub, J. E.; Thirumalai, D. Dynamics of Locking of Peptides onto Growing Amyloid Fibrils. *Proc. Natl. Acad. Sci. U.S.A.* **2009**, *106*, 11948−11953.
(14) Miller, Y.; Ma, B.; Nussinov, R. Polymorphism in Alzheimer Aβ Amyloid Organization Reflects Conformational Selection in a Rugged Energy Landscape. *Chem. Rev.* **2010**, *110*, 4820−4838.
(15) Thirumalai, D.; Reddy, G.; Straub, J. E. Role of Water in Protein Aggregation and Amyloid Polymorphism. *Acc. Chem. Res.* **2012**, *45*, 83−92.
(16) van der Wel, P. C. A.; Lewandowski, J. z. R.; Griffin, R. G. Solid-State NMR Study of Amyloid Nanocrystals and Fibrils Formed by the Peptide GNNQQNY from Yeast Prion Protein Sup35p. *J. Am. Chem. Soc.* **2007**, *129*, 5117−5130.
(17) Shen, C. L.; Murphy, R. M. Solvent Effects on Self-Assembly of Beta-Amyloid Peptide. *Biophys. J.* **1995**, *69*, 640−651.
(18) Tran, H. T.; Mao, A.; Pappu, R. V. Role of Backbone-Solvent Interactions in Determining Conformational Equilibria of Intrinsically Disordered Proteins. *J. Am. Chem. Soc.* **2008**, *130*, 7380−7392.
(19) Krone, M. G.; Hua, L.; Soto, P.; Zhou, R.; Berne, B. J.; Shea, J.-E. Role of Water in Mediating the Assembly of Alzheimer Amyloid-β Aβ16−22 Protofilaments. *J. Am. Chem. Soc.* **2008**, *130*, 11066−11072.
(20) Zheng, J.; Jang, H.; Ma, B.; Tsai, C.-J.; Nussinov, R. Modeling the Alzheimer Aβ_{17-42} Fibril Architecture: Tight Intermolecular Sheet-Sheet Association and Intramolecular Hydrated Cavities. *Biophys. J.* **2007**, *93*, 3046−3057.
(21) Chong, S.-H.; Ham, S. Impact of Chemical Heterogeneity on Protein Self-Assembly in Water. *Proc. Natl. Acad. Sci. U.S.A.* **2012**, *109*, 7636−7641.
(22) Pal, S. K.; Peon, J.; Bagchi, B.; Zewail, A. H. Biological Water: Femtosecond Dynamics of Macromolecular Hydration. *J. Phys. Chem. B* **2002**, *106*, 12376−12395.
(23) Halle, B. Protein Hydration Dynamics in Solution: A Critical Survey. *Philos. Trans. R. Soc., B* **2004**, *359*, 1207−1224.
(24) Bandyopadhyay, S.; Chakraborty, S.; Bagchi, B. Exploration of the Secondary Structure Specific Differential Solvation Dynamics Between the Native And Molten Globule States of the Protein HP-36. *J. Phys. Chem. B* **2006**, *110*, 20629−20634.
(25) Ebbinghaus, S.; Kim, S. J.; Heyden, M.; Yu, X.; Heugen, U.; Gruebele, M.; Leitner, D. M.; Havenith, M. An Extended Dynamical Hydration Shell Around Proteins. *Proc. Natl. Acad. Sci. U.S.A.* **2007**, *104*, 20749−20752.
(26) Li, T.; Hassanali, A. A.; Kao, Y.-T.; Zhong, D.; Singer, S. J. Hydration Dynamics and Time Scales of Coupled Water−Protein Fluctuations. *J. Am. Chem. Soc.* **2007**, *129*, 3376−3382.
(27) Bhattacharyya, K. Nature of Biological Water: A Femtosecond Study. *Chem. Commun.* **2008**, *2850*, 2848−2857.
(28) Sengupta, N.; Jaud, S.; Tobias, D. J. Hydration Dynamics in a Partially Denatured Ensemble of the Globular Protein Human α-Lactalbumin Investigated with Molecular Dynamics Simulations. *Biophys. J.* **2008**, *95*, 5257−5267.
(29) Nandi, N.; Bagchi, B. Dielectric Relaxation of Biological Water. *J. Phys. Chem. B* **1997**, *101*, 10954−10961.
(30) Bagchi, B. Water Dynamics in the Hydration Layer around Proteins and Micelles. *Chem. Rev.* **2005**, *105*, 3197−3219.
(31) Fenimore, P. W.; Frauenfelder, H.; McMahon, B. H.; Parak, F. G. Slaving: Solvent Fluctuations Dominate Protein Dynamics and Functions. *Proc. Natl. Acad. Sci. U.S.A.* **2002**, *99*, 16047−16051.
(32) Frauenfelder, H.; Fenimore, P. W.; Chen, G.; McMahon, B. H. Protein Folding is Slaved to Solvent Motions. *Proc. Natl. Acad. Sci. U.S.A.* **2006**, *103*, 15469−15472.
(33) Tarek, M.; Tobias, D. J. Role of Protein-Water Hydrogen Bond Dynamics in the Protein Dynamical Transition. *Phys. Rev. Lett.* **2002**, *88*, 138101.
(34) Sinha, S. K.; Bandyopadhyay, S. Differential Flexibility of the Secondary Structures of Lysozyme and the Structure and Ordering of Surrounding Water Molecules. *J. Chem. Phys.* **2011**, *134*, 115101.
(35) Sinha, S. K.; Bandyopadhyay, S. Local Heterogeneous Dynamics of Water around Lysozyme: A Computer Simulation Study. *Phys. Chem. Chem. Phys.* **2012**, *14*, 899−913.
(36) Fogarty, A. C.; Laage, D. Water Dynamics in Protein Hydration Shells: The Molecular Origins of the Dynamical Perturbation. *J. Phys. Chem. B* **2014**, *118*, 7715−7729.
(37) Kale, L.; Skeel, R.; Bhandarkar, M.; Brunner, R.; Gursoy, A.; Krawetz, N.; Phillips, J.; Shinozaki, A.; Varadarajan, K.; Schulten, K. NAMD2: Greater Scalability for Parallel Molecular Dynamics. *J. Comput. Phys.* **1999**, *151*, 283−312.
(38) Mackerell, A. D. Empirical Force Fields for Biological Macromolecules: Overview and Issues. *J. Comput. Chem.* **2004**, *25*, 1584−1604.
(39) Mackerell, A. D.; Feig, M.; Brooks, C. L. Extending the Treatment of Backbone Energetics in Protein Force Fields: Limitations of Gas-Phase Quantum Mechanics in Reproducing Protein Conformational Distributions in Molecular Dynamics Simulations. *J. Comput. Chem.* **2004**, *25*, 1400−1415.
(40) MacKerell, A. D.; Bashford, D.; Bellott; Dunbrack, R. L.; Evanseck, J. D.; Field, M. J.; Fischer, S.; Gao, J.; Guo, H.; Ha, S.; Joseph-McCarthy, D.; et al. All-Atom Empirical Potential for Molecular Modeling and Dynamics Studies of Proteins. *J. Phys. Chem. B* **1998**, *102*, 3586−3616.
(41) Jorgensen, W. L.; Chandrasekhar, J.; Madura, J. D.; Impey, R. W.; Klein, M. L. Comparison of Simple Potential Functions for Simulating Liquid Water. *J. Chem. Phys.* **1983**, *79*, 926−935.
(42) Feller, S. E.; Zhang, Y.; Pastor, R. W.; Brooks, B. R. Constant Pressure Molecular Dynamics Simulation: The Langevin Piston Method. *J. Chem. Phys.* **1995**, *103*, 4613−4621.
(43) Ryckaert, J.-P.; Ciccotti, G.; Berendsen, H. J. C. Numerical Integration of the Cartesian Equations of Motion of a System with Constraints: Molecular Dynamics of N-Alkanes. *J. Comput. Phys.* **1977**, *23*, 327−341.
(44) Essmann, U.; Perera, L.; Berkowitz, M. L.; Darden, T.; Lee, H.; Pedersen, L. G. A Smooth Particle Mesh Ewald Method. *J. Chem. Phys.* **1995**, *103*, 8577−8593.
(45) Vijay-Kumar, S.; Bugg, C. E.; Cook, W. J. Structure of Ubiquitin Refined at 1.8 Å Resolution. *J. Mol. Biol.* **1987**, *194*, 531−544.
(46) Zhang, S.; Iwata, K.; Lachenmann, M. J.; Peng, J. W.; Li, S.; Stimson, E. R.; Lu, Y. a.; Felix, A. M.; Maggio, J. E.; Lee, J. P. The Alzheimer's Peptide Aβ Adopts a Collapsed Coil Structure in Water. *J. Struct. Biol.* **2000**, *130*, 130−141.
(47) Lee, C.; Ham, S. Characterizing Amyloid-Beta Protein Misfolding from Molecular Dynamics Simulations with Explicit Water. *J. Comput. Chem.* **2011**, *32*, 349−355.
(48) Sgourakis, N. G.; Merced-Serrano, M.; Boutsidis, C.; Drineas, P.; Du, Z.; Wang, C.; Garcia, A. E. Atomic-Level Characterization of the Ensemble of the Aβ (1−42) Monomer in Water Using Unbiased Molecular Dynamics Simulations and Spectral Algorithms. *J. Mol. Biol.* **2011**, *405*, 570−583.
(49) Chong, S.-H.; Yim, J.; Ham, S. Structural Heterogeneity in Familial Alzheimer's Disease Mutants of Amyloid-beta Peptides. *Mol. BioSyst.* **2013**, *9*, 997−1003.
(50) Rosenman, D. J.; Connors, C. R.; Chen, W.; Wang, C.; García, A. E. Aβ Monomers Transiently Sample Oligomer and Fibril-Like Configurations: Ensemble Characterization Using a Combined MD/NMR Approach. *J. Mol. Biol.* **2013**, *425*, 3338−3359.
(51) Miao, Y.; Nichols, S. E.; McCammon, J. A. Free Energy Landscape of G-Protein Coupled Receptors, Explored by Accelerated Molecular Dynamics. *Phys. Chem. Chem. Phys.* **2014**, *16*, 6398−6406.
(52) Okamoto, A.; Yano, A.; Nomura, K.; Higai, S. i.; Kurita, N. Stable Conformation of Full-Length Amyloid-β (1−42) Monomer in Water: Replica Exchange Molecular Dynamics and Ab Initio Molecular Orbital Simulations. *Chem. Phys. Lett.* **2013**, *577*, 131−137.
(53) Olubiyi, O. O.; Strodel, B. Structures of the Amyloid β-Peptides Aβ_{1-40} and Aβ_{1-42} as Influenced by pH and a D-Peptide. *J. Phys. Chem. B* **2012**, *116*, 3280−3291.
(54) Sugita, Y.; Okamoto, Y. Replica-Exchange Molecular Dynamics Method for Protein Folding. *Chem. Phys. Lett.* **1999**, *314*, 141−151.
(55) Hamelberg, D.; de Oliveira, C. A. F.; McCammon, J. A. Sampling of Slow Diffusive Conformational Transitions with

Accelerated Molecular Dynamics. *J. Chem. Phys.* **2007**, *127*, 155102−155109.
(56) Hamelberg, D.; Mongan, J.; McCammon, J. A. Accelerated Molecular Dynamics: A Promising and Efficient Simulation Method for Biomolecules. *J. Chem. Phys.* **2004**, *120*, 11919−11929.
(57) Markwick, P. R. L.; McCammon, J. A. Studying Functional Dynamics in Bio-Molecules Using Accelerated Molecular Dynamics. *Phys. Chem. Chem. Phys.* **2011**, *13*, 20053−20065.
(58) Strodel, B.; Lee, J. W. L.; Whittleston, C. S.; Wales, D. J. Transmembrane Structures for Alzheimer's $A\beta_{1-42}$ Oligomers. *J. Am. Chem. Soc.* **2010**, *132*, 13300−13312.
(59) Humphrey, W.; Dalke, A.; Schulten, K. VMD: Visual Molecular Dynamics. *J. Mol. Graphics* **1996**, *14*, 33−38.
(60) Sisodia, S. S. Beta-Amyloid Precursor Protein Cleavage by a Membrane-Bound Protease. *Proc. Natl. Acad. Sci. U.S.A.* **1992**, *89*, 6075−6079.
(61) Baumketner, A.; Bernstein, S. L.; Wyttenbach, T.; Bitan, G.; Teplow, D. B.; Bowers, M. T.; Shea, J.-E. Amyloid B-Protein Monomer Structure: A Computational and Experimental Study. *Protein Sci.* **2006**, *15*, 420−428.
(62) Luhrs, T.; Ritter, C.; Adrian, M.; Riek-Loher, D.; Bohrmann, B.; Dobeli, H.; Schubert, D.; Riek, R. 3D Structure of Alzheimer's Amyloid-β (1−42) Fibrils. *Proc. Natl. Acad. Sci. U.S.A.* **2005**, *102*, 17342−17347.
(63) Khandogin, J.; Brooks, C. L. Linking Folding with Aggregation in Alzheimer's β-amyloid Peptides. *Proc. Natl. Acad. Sci. U.S.A.* **2007**, *104*, 16880−16885.
(64) Chatterjee, P.; Sengupta, N. Effect of the A30P Mutation on the Structural Dynamics of Micelle-Bound αSynuclein Released in Water: A Molecular Dynamics Study. *Eur. Biophys. J.* **2012**, *41*, 483−489.
(65) Jose, J.; Sengupta, N. Molecular Dynamics Simulation Studies of the Structural Response of an Isolated Aβ1−42 Monomer Localized in the Vicinity of the Hydrophilic TiO_2 Surface. *Eur. Biophys. J.* **2013**, *42*, 487−494.
(66) Jana, A. K.; Jose, J. C.; Sengupta, N. Critical Roles of Key Domains in Complete Adsorption of Aβ Peptide on Single-Walled Carbon Nanotubes: Insights with Point Mutations and MD Simulations. *Phys. Chem. Chem. Phys.* **2013**, *15*, 837−844.
(67) Jana, A. K.; Sengupta, N. Adsorption Mechanism and Collapse Propensities of the Full-Length, Monomeric Aβ1−42 on the Surface of a Single-Walled Carbon Nanotube: A Molecular Dynamics Simulation Study. *Biophys. J.* **2012**, *102*, 1889−1896.
(68) Sinha, S. K.; Chakraborty, S.; Bandyopadhyay, S. Thickness of the Hydration Layer of a Protein from Molecular Dynamics Simulation. *J. Phys. Chem. B* **2008**, *112*, 8203−8209.
(69) Bizzarri, A. R.; Cannistraro, S. Molecular Dynamics of Water at the Protein-Solvent Interface. *J. Phys. Chem. B* **2002**, *106*, 6617−6633.
(70) Chong, S.-H. Connections of Activated Hopping Processes with the Breakdown of the Stokes-Einstein Relation and with Aspects of Dynamical Heterogeneities. *Phys. Rev. E* **2008**, *78*, 041501.
(71) Flenner, E.; Szamel, G. Relaxation In a Glassy Binary Mixture: Mode-Coupling-Like Power Laws, Dynamic Heterogeneity, and a New Non-Gaussian Parameter. *Phys. Rev. E* **2005**, *72*, 011205.
(72) Rocchi, C.; Bizzarri, A. R.; Cannistraro, S. Water Dynamical Anomalies Evidenced by Molecular-Dynamics Simulations at the Solvent-Protein Interface. *Phys. Rev. E* **1998**, *57*, 3315−3325.
(73) Pizzitutti, F.; Marchi, M.; Sterpone, F.; Rossky, P. J. How Protein Surfaces Induce Anomalous Dynamics of Hydration Water. *J. Phys. Chem. B* **2007**, *111*, 7584−7590.
(74) Pal, S.; Bandyopadhyay, S. Importance of Protein Conformational Motions and Electrostatic Anchoring Sites on the Dynamics and Hydrogen Bond Properties of Hydration Water. *Langmuir* **2013**, *29*, 1162−1173.
(75) Uversky, V. N.; Dunker, A. K. Understanding Protein Non-Folding. *Biochim. Biophys. Acta* **2010**, *1804*, 1231−1264.
(76) Allen, M. P.; Tidlesley, D. J. *Computer Simulation of Liquids*; Clarendon: Oxford, 1987.
(77) Stillinger, F. H. Theory and Molecular Models for Water. *Adv. Chem. Phys.* **1975**, *31*, 1−101.
(78) Stillinger, F. H. Water Revisited. *Science* **1980**, *209*, 451−457.
(79) Luzar, A.; Chandler, D. Hydrogen-Bond Kinetics in Liquid Water. *Nature* **1996**, *379*, 55−57.
(80) Luzar, A. Resolving The Hydrogen Bond Dynamics Conundrum. *J. Chem. Phys.* **2000**, *113*, 10663−10675.
(81) Luzar, A. Extent of Inter-Hydrogen Bond Correlations in Water. Temperature Effect. *Chem. Phys.* **2000**, *258*, 267−276.
(82) Luzar, A.; Chandler, D. Effect of Environment on Hydrogen Bond Dynamics in Liquid Water. *Phys. Rev. Lett.* **1996**, *76*, 928−931.
(83) Stillinger, F. H.; Rahman, A. Improved Simulation of Liquid Water by Molecular Dynamics. *J. Chem. Phys.* **1974**, *60*, 1545−1557.
(84) Mezei, M.; Beveridge, D. L. Theoretical Studies of Hydrogen Bonding in Liquid Water and Dilute Aqueous Solutions. *J. Chem. Phys.* **1981**, *74*, 622−632.
(85) Luzar, A.; Chandler, D. Structure and Hydrogen Bond Dynamics of Water-Dimethyl Sulfoxide Mixtures by Computer Simulations. *J. Chem. Phys.* **1993**, *98*, 8160−8173.
(86) Rahman, A.; Stillinger, F. H. Molecular Dynamics Study of Liquid Water. *J. Chem. Phys.* **1971**, *55*, 3336−3359.
(87) Rapaport, D. C. Hydrogen Bonds in Water Network Organization and Lifetimes. *Mol. Phys.* **1983**, *50*, 1151−1162.
(88) Sarupria, S.; Garde, S. Quantifying Water Density Fluctuations and Compressibility of Hydration Shells of Hydrophobic Solutes and Proteins. *Phys. Rev. Lett.* **2009**, *103*, 037803.
(89) Patel, A.; Varilly, P.; Chandler, D.; Garde, S. Quantifying Density Fluctuations in Volumes of All Shapes and Sizes Using Indirect Umbrella Sampling. *J. Stat. Phys.* **2011**, *145*, 265−275.
(90) Patel, A. J.; Varilly, P.; Jamadagni, S. N.; Hagan, M. F.; Chandler, D.; Garde, S. Sitting at the Edge: How Biomolecules Use Hydrophobicity to Tune Their Interactions and Function. *J. Phys. Chem. B* **2012**, *116*, 2498−2503.
(91) Chong, S.-H.; Ham, S. Atomic-Level Investigations on the Amyloid-β Dimerization Process and its Driving Forces in Water. *Phys. Chem. Chem. Phys.* **2012**, *14*, 1573−1575.
(92) Chong, S.-H.; Ham, S. Atomic Decomposition of the Protein Solvation Free Energy and its Application to Amyloid-Beta Protein in Water. *J. Chem. Phys.* **2011**, *135*, 034506.